INJURIES AND KINEMATICS: RESPONSE OF THE CERVICAL SPINE IN INVERTED IMPACTS

Carolyn Roberts
Jason R. Kerrigan
University of Virginia, Center for Applied Biomechanics
United States of America

Paper Number 15-0432

ABSTRACT

Given the frequency and severity of cervical spine injuries resulting from rollover crashes, it is critical to analyze the mechanism of cervical spine injury in this loading condition. In rollover crashes, roof-to-ground impacts can generate axial compression of the cervical spine, which can result in paralysis and death. This study was performed to compare injury type and severity between component and full body inverted vertex impact tests with post-mortem human surrogates (PMHS); a secondary aim was to determine how changes in vertebral kinematics resulted in changes in hear reaction loads. Five PMHS were suspended in an inverted seated position and then dropped from two heights to achieve 2 m/s (one subjects once and another twice) and 4.4 m/s (all subjects) at impact. The subjects were dropped on a padded five-axis load cell to record the reaction force from impact. Each PMHS was instrumented with three blocks (each containing three accelerometers and three angular rate sensors) rigidly mounted along the upper thoracic spine and on the head. Injuries were determined using both CT scans and dissection following testing. Vertical force traces from the load cell reflect a similar two peak shape seen in previous full-body and component tests. High-speed (1000 Hz) X-ray video analysis shows the neck retains in its initial orientation but becomes increasingly compressed during the loading portion of the first peak. At the first peak, the cervical spine begins to curve, putting the cervical spine into extension, with the center of curvature around C3 or C4, and continues into bending during the unloading of the first peak. The head then translates forward and the neck moves into flexion during the second peak. Each PMHS achieved a flexion injury in the upper thoracic spine or the lower cervical spine during the testing, which occurred during the second peak of the force trace, contradicting previous theories that injury occurs at the first peak, where maximum force occurs. These tests suggest that the direction of torso loading, impact velocity, and boundary conditions at the ends of the cervical spine all affect the kinematics during impact as well as the resulting injuries, and should all be taken into account when determining appropriate injury criteria and developing biofidelic ATDs to predict injuries in crash tests.

INTRODUCTION

Occupant-to-roof impact can cause some of the most severe injuries in rollover crashes; these injuries have been shown to be related to the amount of roof intrusion into the occupant compartment and the post-crash headroom in the vehicle (Ridella et al. 2008). Occupant-roof interaction generates axial compression in the cervical spine, which is responsible for many rollover crash-induced injuries. Although there are multiple head-neck PMHS compoment studies focused on cervical spine injuries caused by axial compression, few full-body PMHS tests have been performed (Sances et al., 1981; Nusholtz, 1983; Yoganandan et al., 1991; Kerrigan et al. 2014). Viano combines the data from studies by Sances, Nusholtz, and Yoganandan and reports full-body PMHS testing consistently produced injury above 4.0 m/s and consistently resulted in no injury below 2.0 m/s, and more data is needed between the 2.0 and 4.0 m/s range (Sances et al., 1981; Nusholtz, 1983; Yoganandan et al., 1991; Viano & Parenteau , 2008).

Previous head-neck component vertex-impact testing that employed a fixed torso mass (16 kg) and a constraint on the motion of the T1 vertebra has produced severe injury at or above 3.1 m/s (Nightingale et al. 1996, 1997). A more recent study escrived vertex impacr experiments with four full-body PMHS in an impact conditions between 3.0 amd 3.6 m/s, with a goal of generating the same impact positioning and condition achieved by Nightingale in component testing (Nightingale et al. 1996, 1997; Kerrigan et al. 2014). These velocity conditions were also chosen in order to help fill the void of data identified by Viano and Parenteau (Viano & Parenteau 2008). However, the

study found that injuries were significantly less severe than in the Nightingale studies, with only one fracture in the full-body drop tests related to the first 100 ms after impact, and hypothesized these differences in injury severity were due to contraints on T1 (Nightingale et al., 1996, 1997).

This study aimed to expand on the study by Kerrigan et al. (2014) by subjecting five more PMHS to inverted vertex impact. Conditions were the same as the previous study, but tests were performed at 2.0 and 4.4 m/s to compare the results of these recent whole body tests to those of the literature ((Sances et al., 1981; Nusholtz, 1983; Yoganandan et al., 1991) that utilized similar velocities. Specific aims of the cyrrent study included determination whether injuries, in general, can be produced when impact velocity is 4.4 m/s, comparison of injury severity and type to those recorded in previous component and whole body tests, and to identify how abrupt changes in vertebral kinematics are represented in impact force data.

TESTING METHODS

Five male PMHS were selected for this study; while all subjects were tested with a 4.4 m/s impact velocity; two subjects were tested at 2 m/s to examine the effect of impact velocity on spinal dynamics and repeatability of response (Table 1).

Table 1.
Physical information and test matrix for each post-mortem human surrogate (PMHS) tested.

Subject Number	Age (years)	Height (mm)	Weight (kg)	Bone Density (DXA)	First Test (Impact Velocity)	Second Test (Impact Velocity)	Third Test (Impact Velocity)
#582	71	1780	68.04	0.8	4.4 m/s (Test 6)	-	-
#534	71	1715	93.16	0.8	2.0 m/s (Test 7)	4.4 m/s (Test 8)	
#606	62	1803	51.71	-0.3	2.0 m/s (Test 9)	2.0 m/s (Test 10)	4.4 m/s (Test 11)
#610	48	1721	61.69	-2.6	4.4 m/s (Test 12)	-	-
#693	47	1780	64.49	-1.3	4.4 m/s (Test 13)	-	-

PMHS Preparation and Instrumentation

The PMHS were obtained and treated in accordance with the ethical guidelines established by the Human Usage Review Panel of the National Highway Traffic Safety Administration, and all testing and handling procedures were reviewed and approved by the Center for Applied Biomechanics Biological Protocol Committee and an independent Oversight Committee at the University of Virginia.

PMHS Preparation The upper extremities of each subject were removed at the sternoclavicular joint. Mounting plates for instrumentation cubes were screwed into the right and left sides of the parietal bones using wood screws. Three sets of mounting hardware were screwed into T1, T4, and T8, and static x-rays and geometric calculations were used to confirm that each mount was rigidly attached to the correct vertebra. After surgical preparation, each subject was wrapped in a thin layer of mechanically adhesive wrap (Coban, 3M, St. Paul, MN, USA) and outfitted with a tactical body harness (355 Extraction Harness, Yates Gear Inc, Redding, CA, USA). A post-preparation CT scan was taken to ensure no damage was done to the cervical spine and to confirm mount locations.

Instrumentation The instrumentation on the spine consisted of three blocks, rigidly attached to T1, T4, and T8 with the mounting hardware. Each block allowed for the attachment of three accelerometers (7264B-2000, Endevco, San Juan Capistrano, CA, USA) and three angular rate sensors (ARS-8K, DTS, Seal Beach, CA, USA). Two more of instrumentation blocks were also affixed to either side of the head onto the mounting plates. Other instrumentation used in the test included two load cells; one padded six-axis load cell (Denton B-3868-D, Humanetics Innovative Solutions, Plymouth, MI, USA) onto which the subjects landed, and another cable load cell that allowed for determination of drop release time. On the top plate of the six-axis load cell, a piece of 25.4 mm thick light-density closed-cell, polyvinyl chloride general purpose foam (V700 Series 1.00", Gaska Tape Inc., Elkhart, IN, USA), was adhered to the steel plate. This foam was used previously (Frechede et al. 2009) to mimic the foam used by Nightingale et al. (1996).

Testing Area Setup and Procedures

Each subject was suspended in an upside-down seated position (Manary et al., 1998) using a system of strings and taut ties (small plastic pieces to adjust the length of each string). All of the strings were looped around a single carabineer, from which the cadaver was suspended. Multiple strings allowed for control over the position, and the subject's torso was rotated until the superior endplate of T1 was oriented at a 25 degree angle from parallel to ground, and the cervical spine was flexed until the Frankfurt plane was oriented parallel to the ground (Nightingale et al., 1996). The subject was positioned such that vertex of the head was centered over the padded load cell. Following final positioning, a ROMER arm scanner (ROMER Absolute Arm with Integrated Scanner, Hexagon Metrology, North Kingstown, RI, USA) was used to collect the orientation and position of all of the accelerometers, angular rate sensors, and the padded load cell onto which each subject landed. After recording this final position with the scans, the subject was released with a solenoid release mechanics to sustain impact with the load plate affixed to the floor.

X-Ray imagery was captured at 1000 Hz in all of the impact tests via positioning the subjects between an image intensifier connected to a high speed digital imager (GX-1, NAC Inc., Japan). Video images were also captured at 1000 Hz from lateral and superior views of the subjects.

A post-test CT was taken, followed by a dissection to confirmed the bony fracture seen in the CT scan and to display ligamentous and facet joint damage.

DATA ANALYSIS

Coordinate Transformations of Data

Head and T1 acceleration data were transformed to local coordinate systems (defined by anatomical landmarks) using the rigid body assumption. The vertebral and head coordinate systems were generated using CT imagery to find the location and orientation of the mount relative to vertebral anatomy. In the vertebral coordinate system, the y-axis was generated by creating a vector from the most lateral point of the left to the most lateral point of the right transverse process. The x-axis was defined to point from the most posterior point of the spinous process to a point on the y-axis such that the x- and y-axes were perpendicular. The z-axis was found by taking the cross product of the x and y vectors. The local head coordinate system was determined using 3 screws (right, left and posterior) that generated the plane in which the cg of the head laid. The y-axis was found by finding the vector of the location of the left screw, L and to the location of the right screw, R. Next the x-axis of the head was determined by finding the perpendicular line to the y-axis on which point P, the posterior of the head, lies. The positive x-axis was found my taking the cross product of the positive x-axis and the positive y-axis. After all of the local data had been found, time histories of the head and T1 local-to-global coordinate system transformations were determined from the angular rate data (Beard & Schlick, 2003).

High Speed X-ray video analysis

Changes to the shape of cervical spine over the first 80 ms (2.0 m/s impact velocity tests) or 175 ms (4.4 m/s impact velocity tests) after impact were determined by tracking the motion of the connection between the vertebral body and the spinous process for each of the cervical vertebrae in each test using X-ray images. The times when abrupt changes in cervical curvature were seen were compared to the head/load plate loads to facilitate dynamic response analysis.

RESULTS AND DISCUSSION

Head Forces

The vertical force traces measured by the padded load cell during impact follow the general double peak shape seen in other studies, both full-body and component, that axially load the cervical spine (Figure 1). Comparing the force results from this test to the previous full-body tests in the literature, the duration, magnitude and peak forces attained during the test closely match (Sances et al., 1981; Nusholtz, 1983; Yoganandan et al., 1991). However, comparing to component tests, increasing the impact velocity by 38% (from 3.2 m/s to 4.4 m/s), resulted in an increased force of 200-250% (Nightingale et al., 1996, 1997). The previous whole body study showed similar peak forces as the component tests, yet no or only subtle injuries (Kerrigan 2014). If this were solely due to rate sensitivity, then it would be at a level that exceeds documented rate sensitivity for all other human tissues. The higher impact force is likely due more of the upper body mass being recruited in the initial impact because there is less time for it to move or articulate away from the load path.

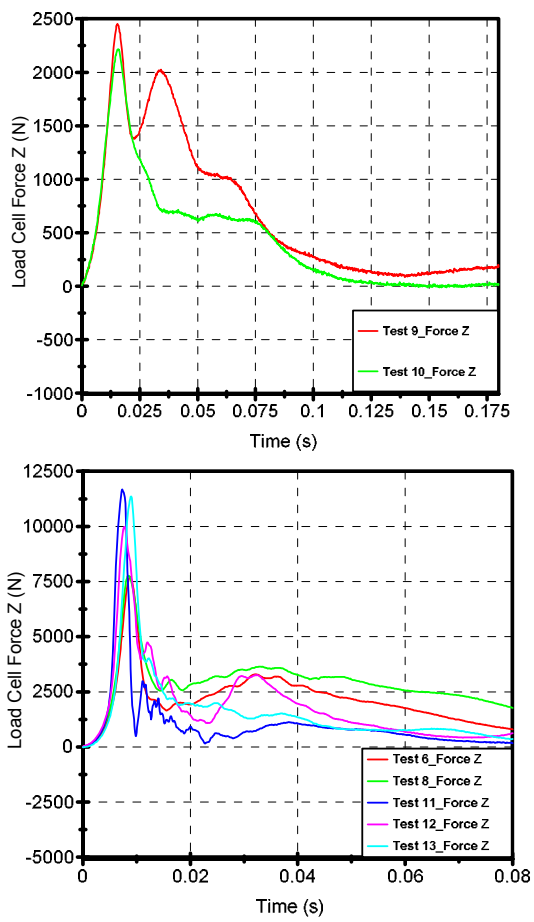

Figure 1. Vertical force traces for each tests. The 2.0 m/s impact velocity tests are depicted in the top graph, and the 4.4 m/s impact velocity tests are depicted in the bottom graph

Kinematics of the torso, neck, and head

Using high-speed X-ray video, it is possible to see the position of the cervical spine as a whole throughout the entire loading period resulting from the impact (both peaks in the vertical force trace). The relative positions of the cervical spine, torso, and head at different times during the vertical force trace are depicted in Figure 2.

In part 1, the PMHS has just initiated contact with the load cell; T1 looks as if it is 25 degrees from horizontal, as it was initially positioned, and the cervical spine is fairly straight with the exception of C1 and C2 (this is probably due to the initial position of the Frankfurt plane at 0 degrees). In part 2, the force trace shows a dramatic increase towards its maximum peak; the cervical spine remains in the same position, but begins to compress slightly. This is the only time during the test where the neck is in pure axial compression. At this time, the torso continues to translate downwards and the head remains fixed in its initial position. In part 3, the maximum Z-force is reached, and the curvature of the neck begins to increase, specifically around C3-C4. In part 4, the vertical force decreases as the neck continues to increase more and more in curvature. In other words, the load decreases at the geometry of the neck changes. In part 5, the vertical force increases once again, and the cervical spine begins to straighten as the head translates forward, and again, the torso continues to translate downward. In part 6, the force reaches a second peak as the neck straightens, and the head continues to translate even further forward, and the torso continues to move down. This puts the neck in shear loading, especially at the C7/T1 interface. In part 7, the Z-force is decreasing, and the bottom of the neck is in flexion with shear loading, the head continues to move forward, and begins to rotate up towards the torso. In 8, the head has almost left the load cell, and the head continues to rotate upwards, while the torso continues to translate downwards and also posteriorly. This rotation and translation of the head continue until the head leaves the load cell and the magnitude of the Z-force is zero.

As was noted before, these general kinematics occurred for every subject with the exception of Subject 582 in Test 6. In Test 6, the Subject's torso loaded the head and neck more vertically. This meant that the head was unable to translate forward and then rotate out of the way of the torso that was loading it.

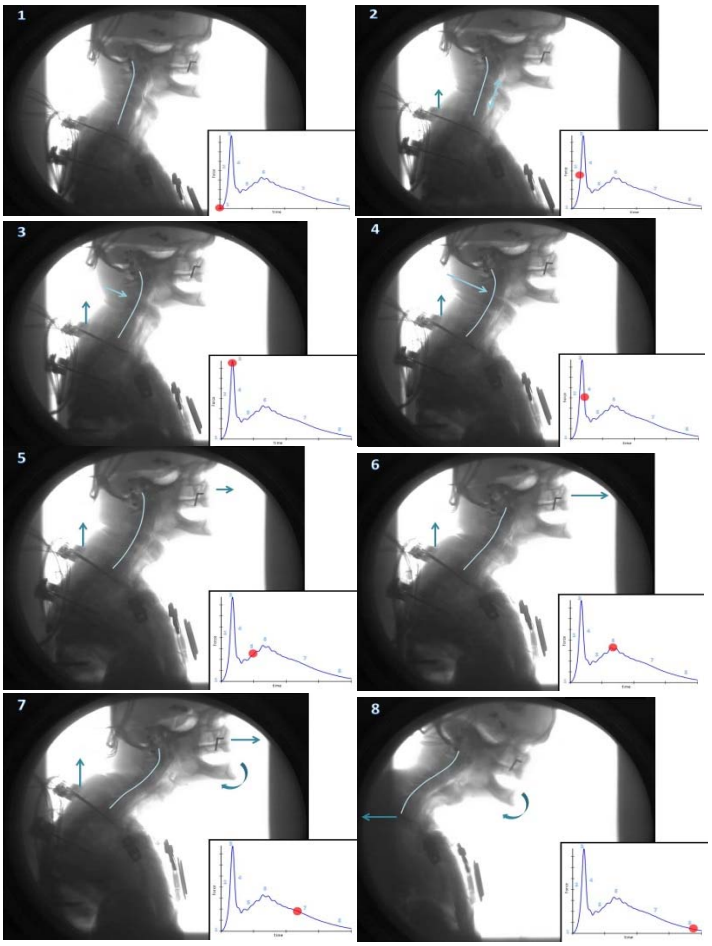

Figure 2. Time step of X-ray video to show the kinematics of the cervical spine with respect to the force trace shape. A light blue curve is drawn along the cervical spine, connecting the location where the spinous process meets the body of each vertebra. Arrows are also shown to depict the general motion of the head and torso of the subject. This figure shows the representative general kinematics that all subjects underwent (with the exception of Subject 582). The red dot on the force trace of each image denotes the relative time at which each motion in the picture is occurring. Each image is also labeled in chronological order (1-8).

Injuries

Table 2 is a collection of the injuries found in all of the subjects. It is very clear that most of the injuries occur in the lower cervical spine and thoracic spine and, it is important to note that only one compression injury in the upper cervical spine was attained during this test. All of the subjects did not attain bony fracture, but all were all injured during testing, most at the 4.4 m/s impact velocity.

Table 2.
Location and type of injuries attained for each subject during testing.

Injury Location ↓	Subject # 582	Subject # 534	Subject # 606	Subject # 610	Subject # 693
C1 Vertebra	Anterior arch fracture				
C2 Vertebra					
C3 Vertebra		Two fractures in the vertebral body			
C3/C4 Joint				Anterior longitudinal ligament tear	
C4 Vertebra					
C5 Vertebra					
C6 Vertebra			Acute fracture of inferior endplate		
C6/C7 Joint				Small tear in anterior longitudinal ligament	
C7 Vertebra			Acute fracture of superior endplate		
C7/T1 Joint		Supraspinous ligament tear Interspinous ligament tear Ligamentum flavum tear	Supraspinous ligament tear Interspinous ligament tear Facet disruption	Supraspinous ligament tear Interspinous ligament tear Ligamentum flavum tear Partial tear of anterior longitudinal ligament Facet disruption	Supraspinous ligament tear Interspinous ligament tear Partial tear of posterior longitudinal ligament
T1 Vertebra	Acute fracture of inferior endplate	Lamina fracture			
T1/T2 Joint					Facet disruption
T2 Vertebra	Acute fracture of inferior endplate Acute fracture of superior endplate	Lamina Fracture			
T3 Vertebra	Acute fracture of superior endplate				
T4 Vertebra		Lamina Fracture			
T5 Vertebra		Lamina Fracture			

Most of the injuries at the C6, C7, T1 and T2 level were located anterior, suggesting they were flexion injuries. Given the mode of injury is flexion, and from the X-ray videos it is clear that the cervical spine does not go into flexion until the second peak of loading, it makes sense that these injuries occur during the second peak of the vertical force trace, not at the point of maximum vertical force. This suggests that simply measuring and then using a maximum force as an injury criterion would not be effective, as these injuries occur nowhere near the maximum force. These injuries are likely due to difference in stiffness between the neck and torso; more motion is allotted for the vertebrae in the cervical spine, and the resistance to motion of the more rigid thoracic spine could cause stress concentrations that resulted in fracture or excessive stretching of ligaments causing tearing.

The ligamentous injuries and fractures in C3 and C4 were located posterior, suggesting their mode of injury was extension. Extension of the cervical spine occurs during the unloading portion of the first peak of the vertical force trace, so it is likely that these extension injuries occurred just following the maximum measured force.

One injury is an outlier to this injury data set: the anterior arch fracture of C1 from subject 582. In the test of this subject, the head was unable to move away from the torso as it descended, and therefore the loading on the cervical spine due to the torso was directed more vertical than in the other tests. As seen in the time step videos in Appendix A, as well as Figure 3 the cervical spine remains straight for a longer portion of the test than in all of the other tests. It is likely that a higher axial force was experienced in the upper cervical spine in test 9, which explains this anterior arch fracture of C1. This injury is likely the only injury resulting from reaching a maximum vertical force where pure axial compression is the only load on the cervical spine.

Subject #606 attained an injury at the C7/T1 joint during test 9, the first 2.0 m/s impact velocity test for this subject. The injury could be seen on the high-speed X-ray video, and occurred after the 175 ms test time. The injury was not initially seen, so Test 10 (at 2.0 m/s impact velocity) and Test 11 (at 4.4 m/s impact velocity) were still performed. The magnitude of Z force between Test 9 and 10 are extremely close, suggesting that the first peak of loading is not affected by the C7/T1 extension injury. There is a distinct difference between the two tests as Test 10 lacks a distinct second peak; there is also a lack of a second peak in Test 11. The lack of the second peak in vertical force coupled with an extension injury further reinforces the idea that flexion injuries occur during the second peak, and that the prior damage to the C7/T1 joint allowed for greater motion between the cervical and thoracic spines, allowing the neck to more easily rotate away from the torso, and decreasing the vertical loading recorded by the load cell.

Differences in kinematics between subjects

Subject 582 had the largest divergence from the generalized kinematics and injuries explained above. Although this subject achieved an axial compression injury, the maximum force in Test 6 has the lowest magnitude of the 4.4 m/s impact velocity tests, yet Subject 582 has the second highest mass. Given all other subjects attained higher maximum forces, but no axial compression injuries, there was likely a difference in position of the cervical spine throughout impact, which could be seen through high speed X-ray imagery (Figure 3). One of the most significant discrepancies is the difference in the head position. In the top image, the head of Subject 582 is trapped almost directly under the torso, whereas in the bottom image, Test 12, the subject's head has translated to the right in the X-ray video, and the neck and torso still have room to translate downwards, because the head has moved out of the way. Another significant difference is the difference between the curvature of the cervical and thoracic spines between the two tests. There is a sharp bend between the cervical and thoracic spines in the bottom figure (the location where Subject 610 attained a flexion injury), whereas the curvature at this location in the top photo is much less severe.

Although the two subjects were initially positioned in the same manner, differences in kinematics and injuries are likely due to geometric differences in the thorax of each subject, which could change the anterior-posterior position of the center of mass of the torso, and thus change the direction of the force that loads the neck.

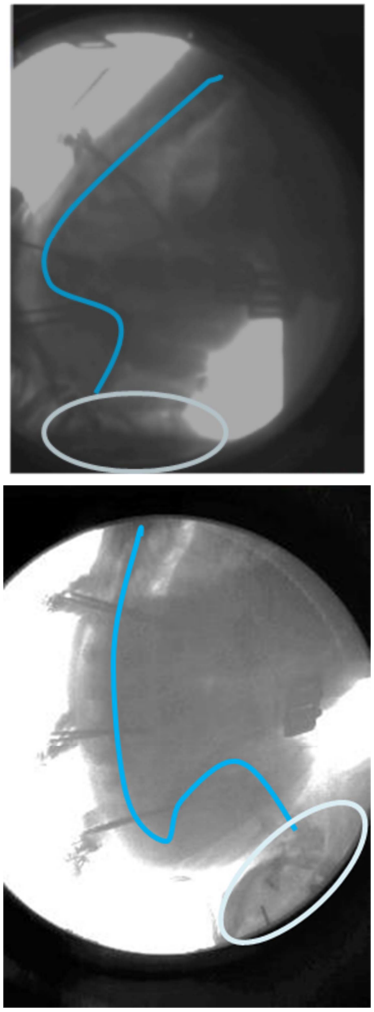

Figure 3. Kinematic differences between the spine and head between Subject 582, Test 6 (top) versus Subject 610, Test 12 (bottom) both at 40ms after impact under the same velocity conditions. The blue line shows a trace of the cervical and thoracic spine shapes and the white circle shows the approximate location and orientation of the head.

Boundary Conditions of the Cervical Spine

It is well established that cervical spine boundary conditions have a substantial effect on the injury tolerance and type in compressive loading (Nightingale et al., 1991). By performing full body-drop tests, one of these boundary effects can be measured in vitro, by measuring the motion of T1 using an instrumentation mount with three accelerometers and three angular rate sensors (Figure 4). There was substantial rotation of the T1 vertebra, especially in the roll (over a 15 degree change).

Given the magnitude of these rotations it is possible that the assumptions made for the boundary conditions by Nightingale in head-neck complex tests. Allowing T1 to only translate in the global Z direction drastically limits the motion that is seen in the full body. By restricting the motion of T1, more severe injuries could have been generated in the cervical spine at a lower impact velocity, and could have been created at different times or different locations than if T1 were allowed to be free to rotate.

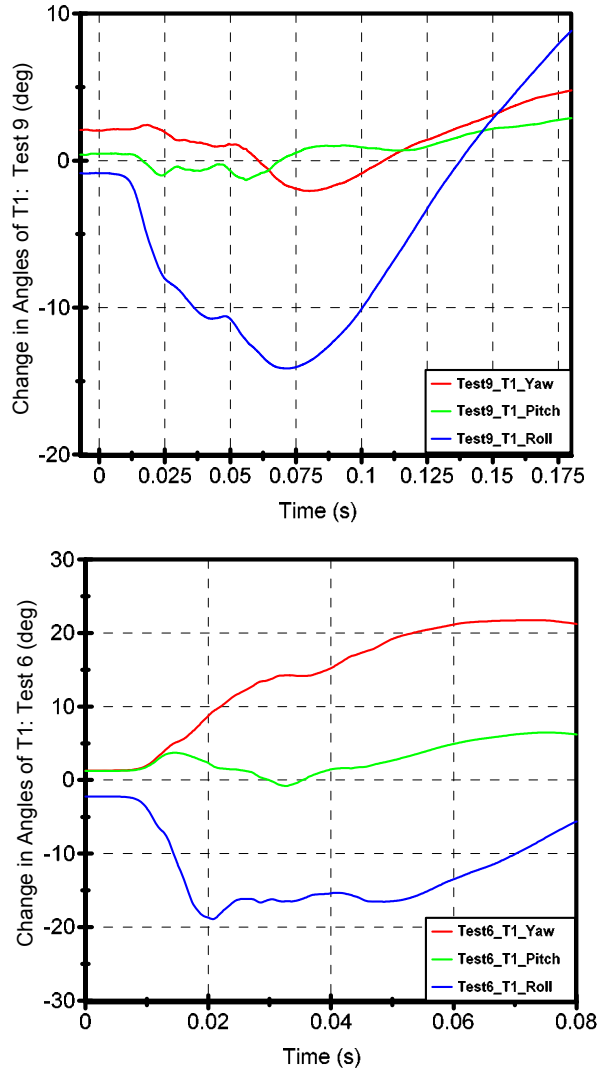

Figure 4. Local vertebral coordinate system angular velocities depicting the motion of T1 during tests are shown. The plot on the top shows the x, y and z angular rates for a 2.0 m/s impact velocity test, and the plot on the bottom shows the same angular rates for a 4.4 m/s impact velocity test.

CONCLUSIONS

Five whole body PMHS were subjected to inverted vertex impacts at 2.0 m/s and 4.4 m/s to examine their response relative to other subjects tested at different velocity tests and component tests that constrained subject motion. The goals of this study included evaluation of whether a 4.4 m/s impact velocity was sufficient to cause injuries, comparison of injury severities and types to those seen in previous tests, and determination of how changes in vertebral kinematics are represented in impact force. The results of this study allowed the following conclusions to be drawn:

Results showed that:

- In general, the PMHS were injured at the 4.4 m/s impact velocity level
- The PMHS injuries generated in these tests were less severe than injuries produced in component test studies conducted at lower impact velocities around 3.2 m/s
- Substantially higher head forces (first peak) were generated in this study than in the previous whole body and component test studies at 3.2 m/s (7500-11500 N vs. 4500 N).

- Injuries, in general, do not occur as a result of the peak impact force; the peak head force does not indicate injury tolerance of the subject
- T1 rotates out of the way during the time period between initial impact, the peak force, and the time when the injury occurs, which suggests that constraining its motion will affect the load response and additionally the injury tolerance of the spine

A next steps in this research could be to evaluate how well existing ATDs represent human respinse by sunjecting ATDs to matched experiments. Aditionally, these data could be used to inform computational analyses aimed at evaluating human body computational models and/or using them to examine the effects of muscle tension on head/neck/torso response.

REFERENCES

[1] Beard, D. A., and Schlick, T. (2003). Unbiased Rotational Moves for Rigid-Body Dynamics. Biophysical Journal, 85, 2973-2976.

[2] Frechede B; McIntosh A; Grzebieta R; Bambach M. (2009) Hybrid III ATD in inverted impacts: influence of impact angle on neck injury risk assessment. Annals of Biomedical Engineering, 37(7): 1403-1414.

[3] Kerrigan, J., Foster, J., Forman, J., Toczyski, J., Roberts, C., Crandall, J. (2014). Axial Compression Injury Tolerance of the Cervical Spine: Initial Results. Traffic Injury Prevention.

[4] Manary M., Reed M., Flannagan C., Schneider L. (1998). ATD Positioning Based on Driver Posture and Position. 42nd Stapp Car Crash Conference. 1-13.

[5] Matsushita T, Sato TB, Hirabayashi K, Fujimura S, Asazuma T, Takatori T. X-ray study of the human neck motion due to head inertia loading. Proceedings of the 38th Stapp Car Crash Conference, 55-64, 1994.

[6] Nightingale RW, Meyers BS, McElhaney J, Richardson WJ, Doherty BJ. (1991) The Influence of End Condition of Human Cervical Spine Injury Mechanisms. SAE 912915, Society of Automotive Engineers.

[7] Nightingale R., McElhaney J., Richardson W., Myers B. (1996). Dynamic responses of the head and cervical spine to axial impact loading. J Biomechanics, 29: 307–18.

[8] Nightingale R., McElhaney J., Camacho D., Kleinberger M., Winkelstein B., Myers B. (1997) The dynamic responses of the cervical spine: buckling, end conditions, and tolerance in compressive impacts. Proceedings of the 41st Stapp Car Crash Conference. Paper number 973344. 451-71.

[9] Nusholtz, G.., et al. (1983). Cervical spine injury mechanisms. No. 831616. SAE Technical Paper.

[10] Ridella, S., and A. Eigen. "Biomechanical investigation of injury mechanisms in rollover crashes from the CIREN database." proceedings of the 2008 International IRCOBI Conference, Bern, Switzerland. 2008.

[11] Sances Jr A, Myklebust J, Cusick JF, Weber R, Houterman C, Larson, SJ, Walsh P, Chilbert M, Prieto T, Zyvoloski M, Ewing C, Thomas D. (1981) Experimental Studies of Brain and Neck Injury. Proceedings of the 25th Stapp Car Crash Conference, Society of Automotive Engineers.

[12] Viano D., Parenteau C. (2008). Analysis of head impacts causing neck compression injury. Traffic Injury Prevention, 9(2):144-52.

[13] Yoganandan N, Pintar FA, Sances A Jr and Maiman DJ. (1991) Strength and kinematic response of dynamic cervical spine injuries, Spine, Vol. 16, No. 10S, pp. 511–517.

APPENDIX A: STILL FRAME IMAGES OF TEST VIDEO

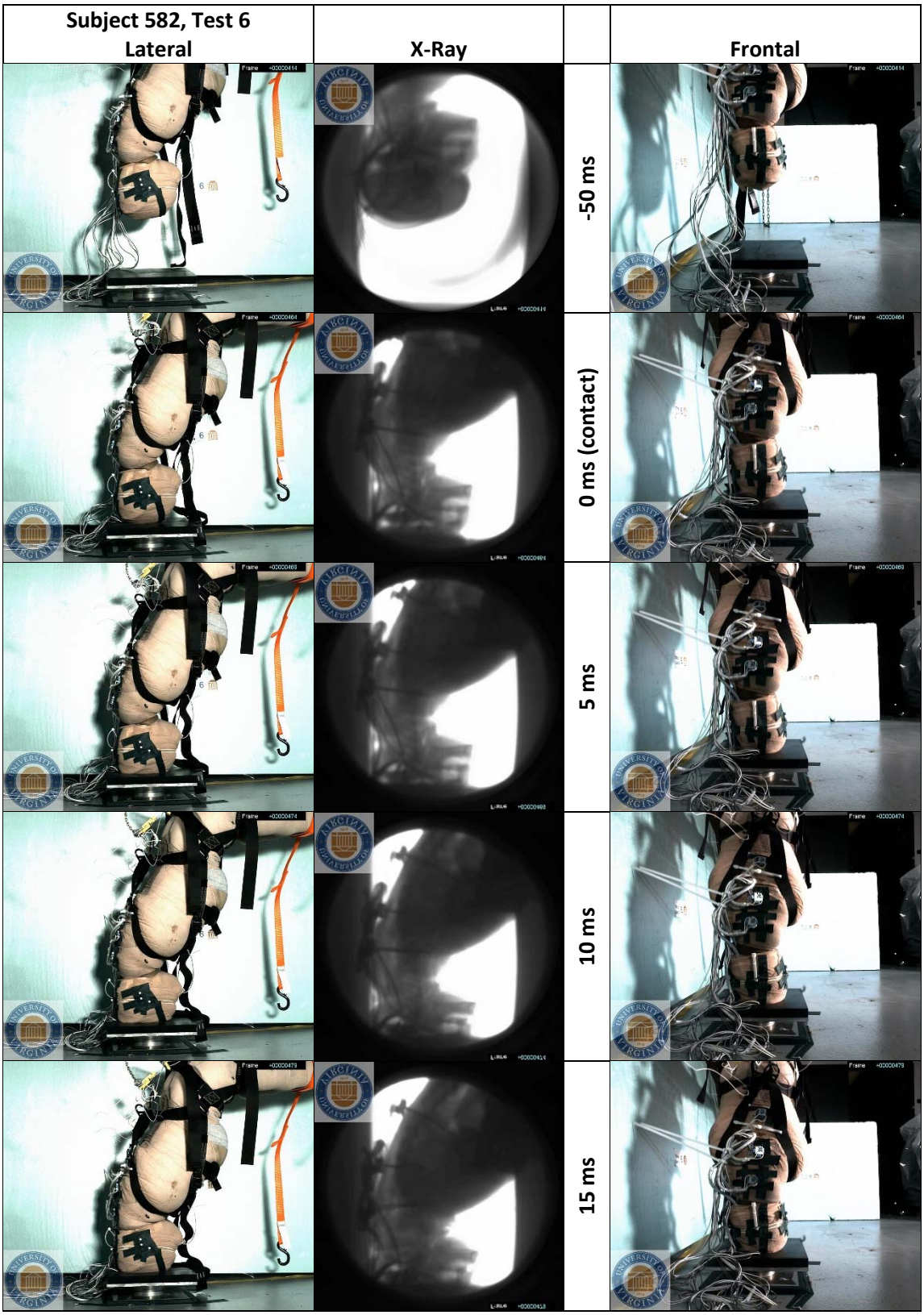

Subject 582, Test 6 Lateral	X-Ray		Frontal
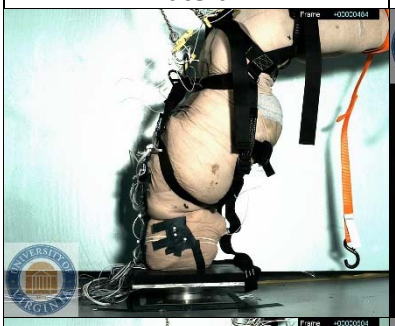		20 ms	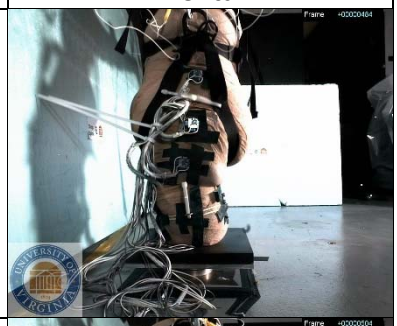
		40 ms	
	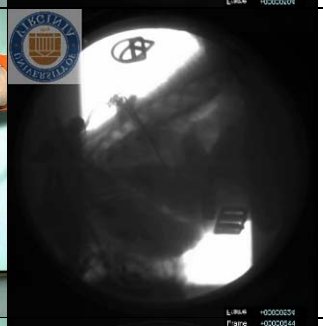	60 ms	
		80 ms	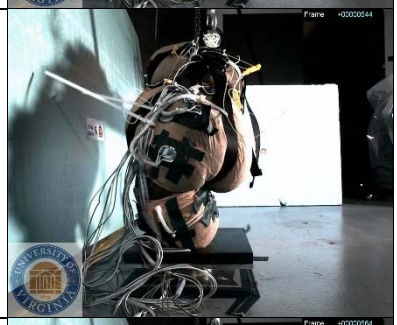
		100 ms	

Subject 534, Test 8 Lateral		Frontal
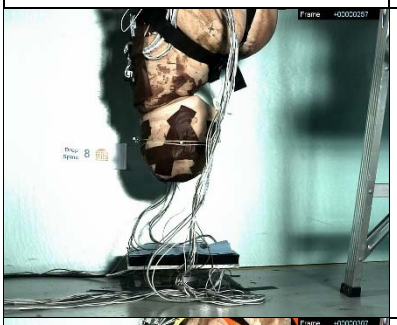	-50 ms	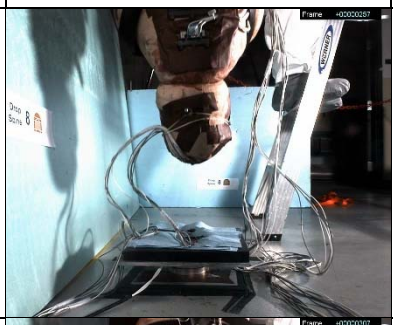
	0 ms (contact)	
	5 ms	
	10 ms	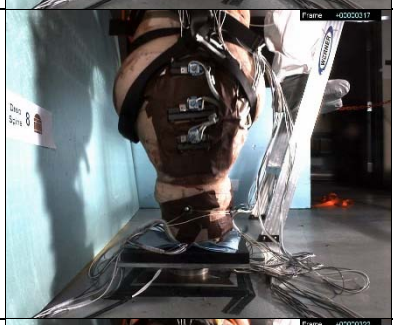
	15 ms	

Subject 534, Test 8 Lateral		Frontal
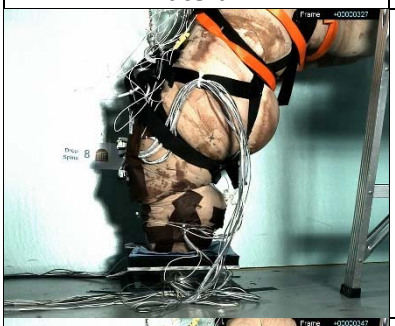	20 ms	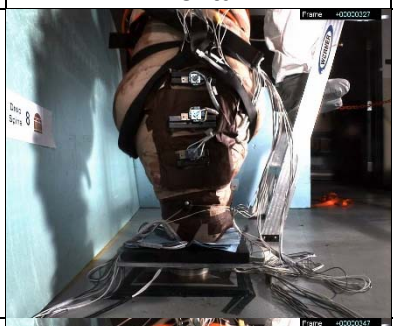
	40 ms	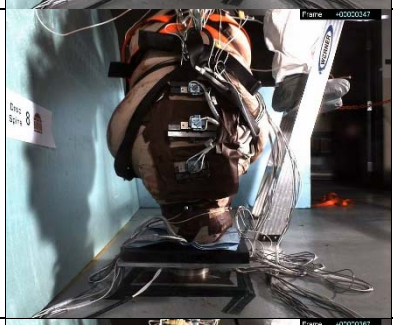
	60 ms	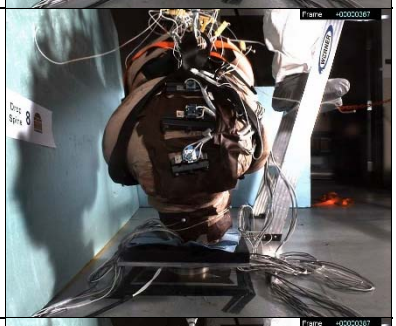
	80 ms	
	100 ms	

Subject 606, Test 9 Lateral	X-Ray		Frontal
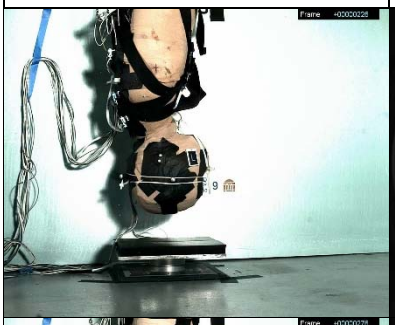		-50 ms	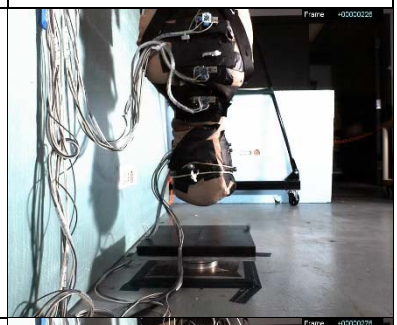
		0 ms (contact)	
		5 ms	
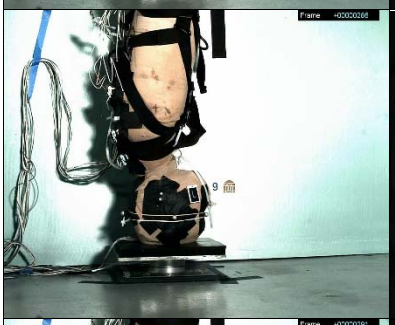		10 ms	
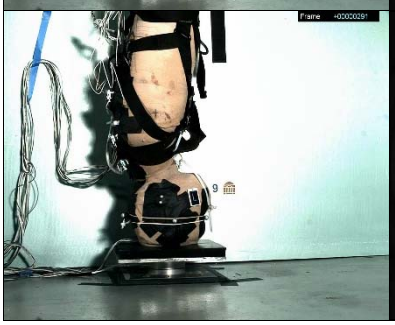		15 ms	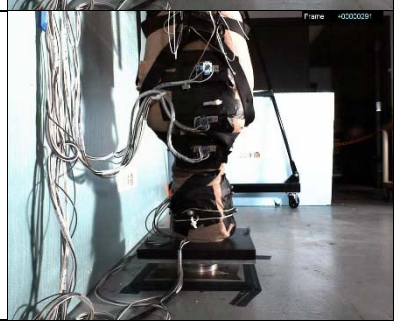

Subject 606, Test 9 Lateral	X-Ray		Frontal
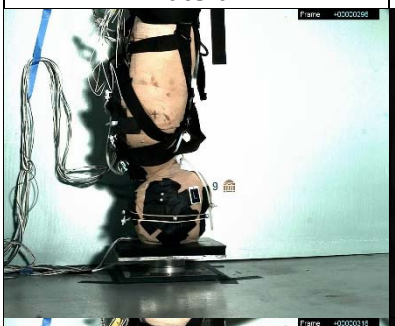		20 ms	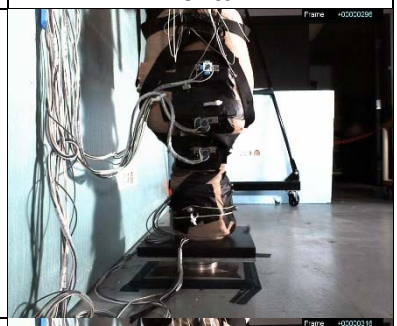
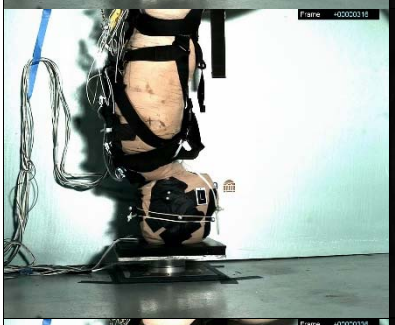	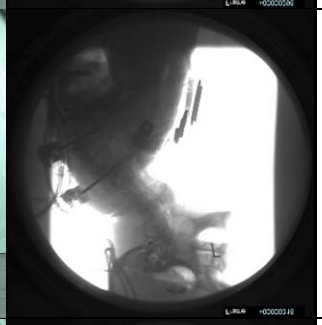	40 ms	
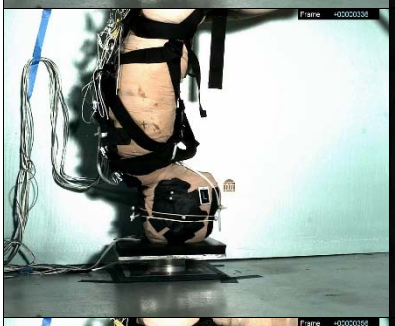		60 ms	
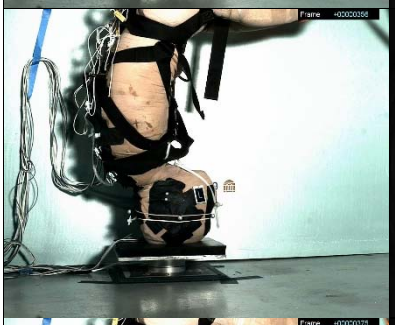	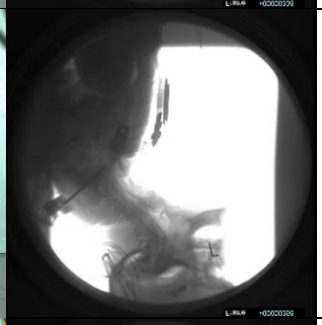	80 ms	
		100 ms	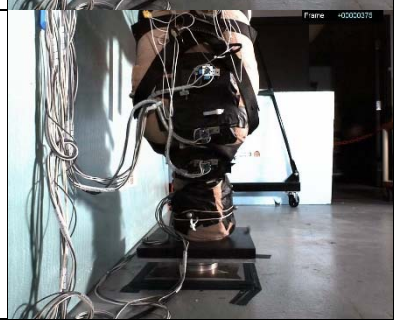

Subject 606, Test 10 Lateral	X-Ray		Frontal
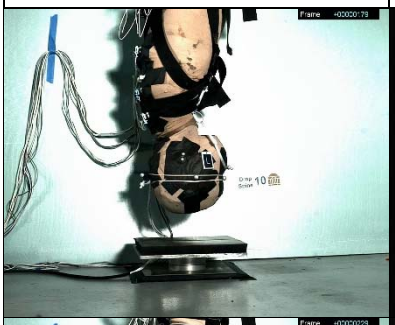	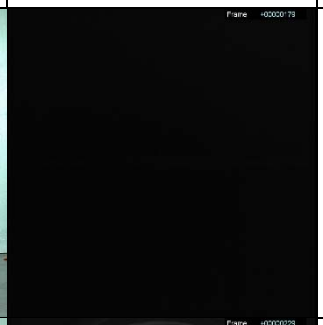	-50 ms	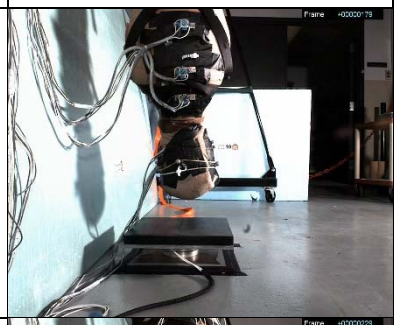
		0 ms (contact)	
		5 ms	
		10 ms	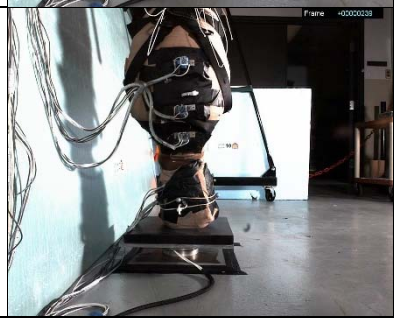

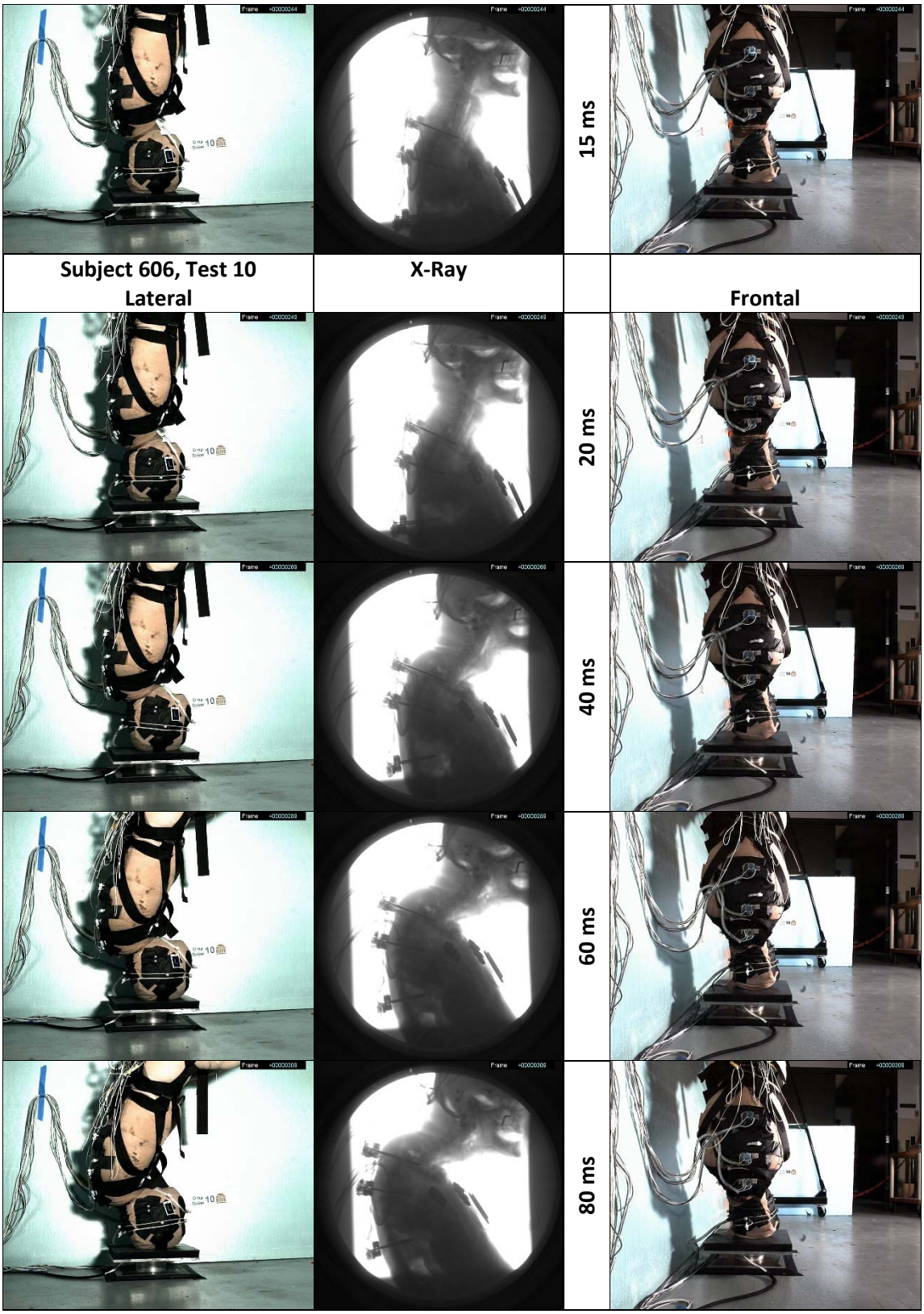
Subject 606, Test 10
Lateral
X-Ray
Frontal
15 ms
20 ms
40 ms
60 ms
80 ms

Subject 606, Test 11 Lateral	X-Ray		Frontal
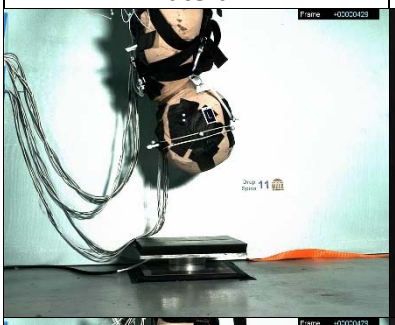		-50 ms	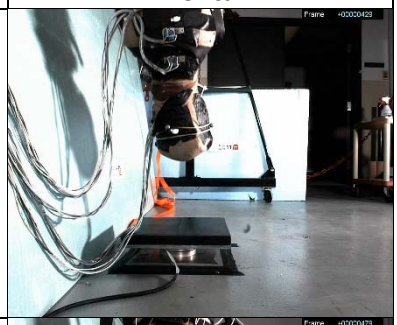
		0 ms (contact)	
		5 ms	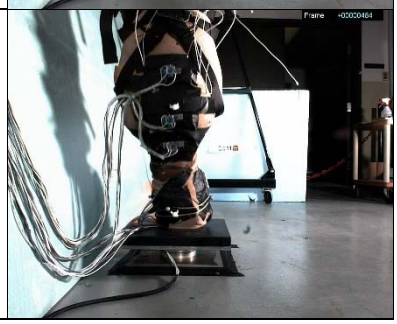

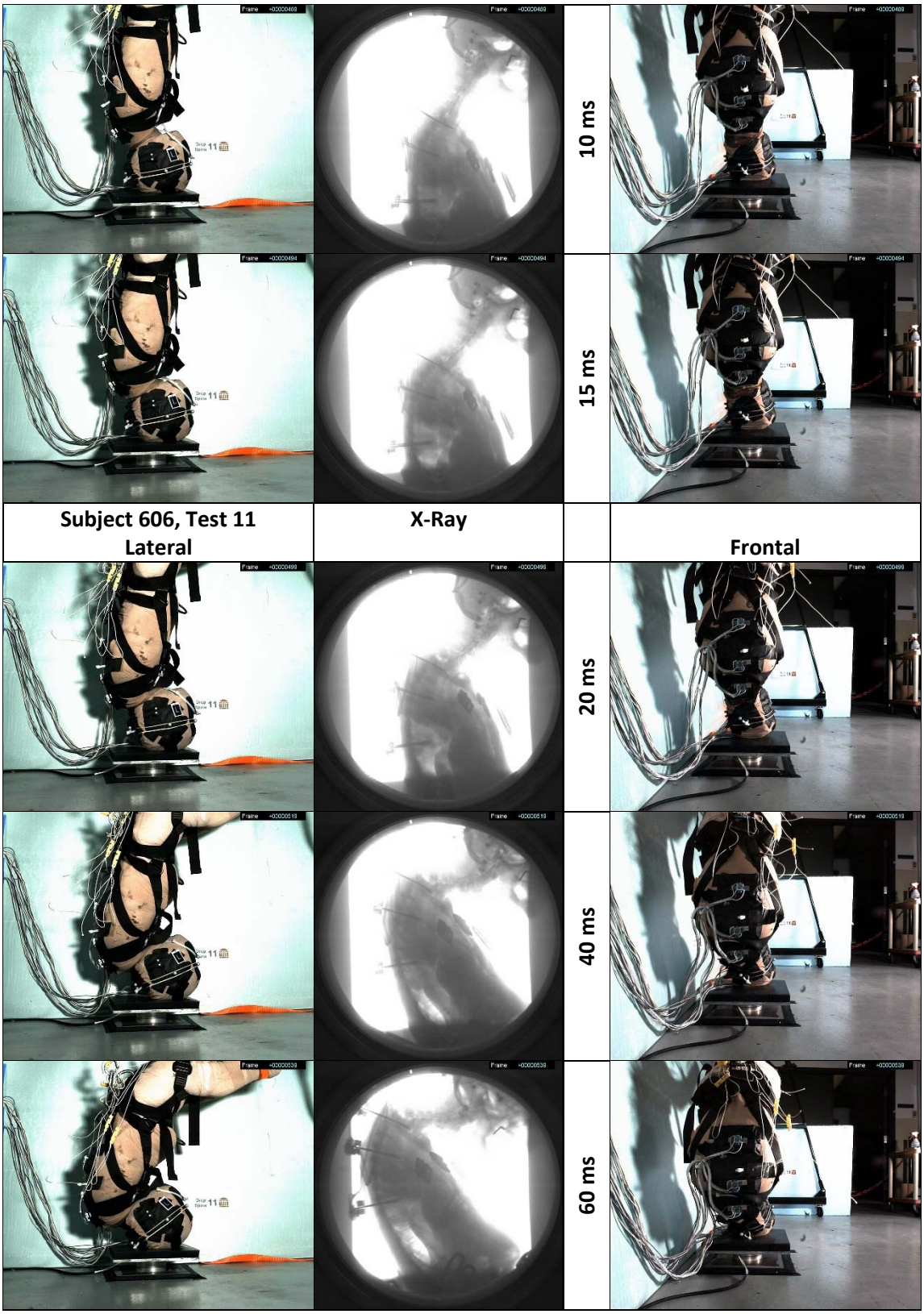
10 ms
15 ms
Subject 606, Test 11
Lateral
X-Ray
Frontal
20 ms
40 ms
60 ms

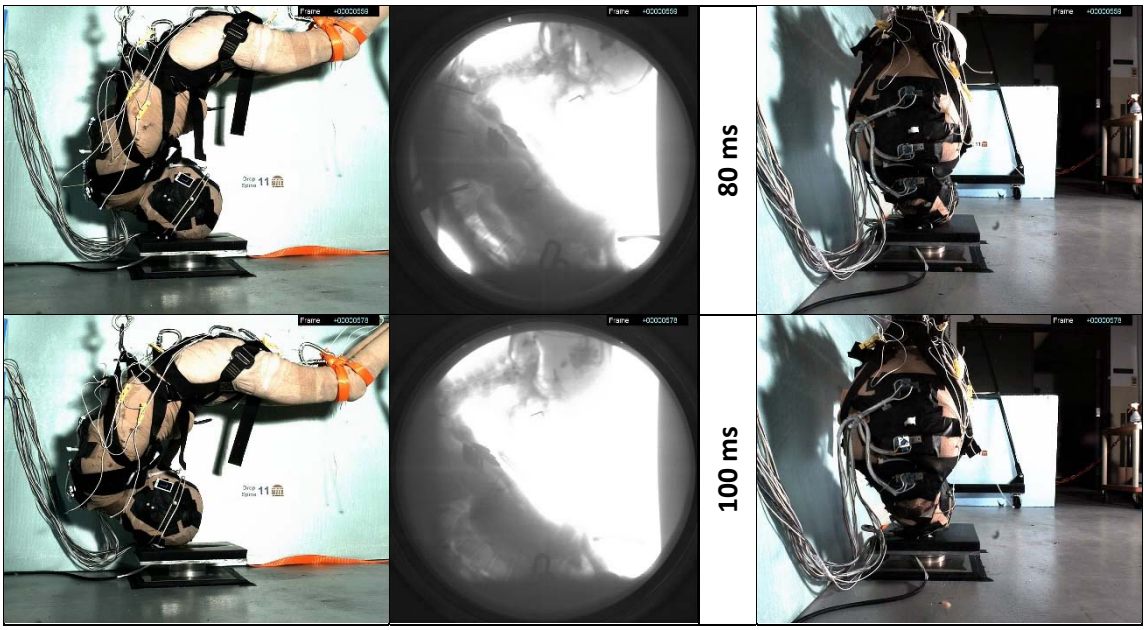
80 ms
100 ms

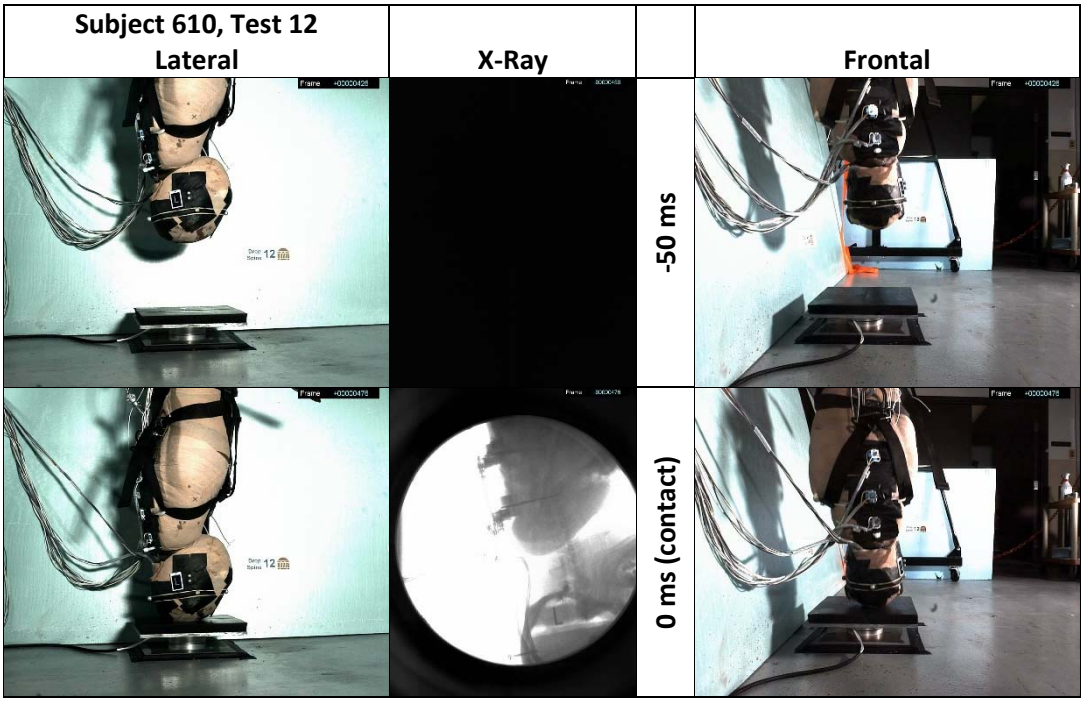
Subject 610, Test 12
Lateral
X-Ray
Frontal
-50 ms
0 ms (contact)

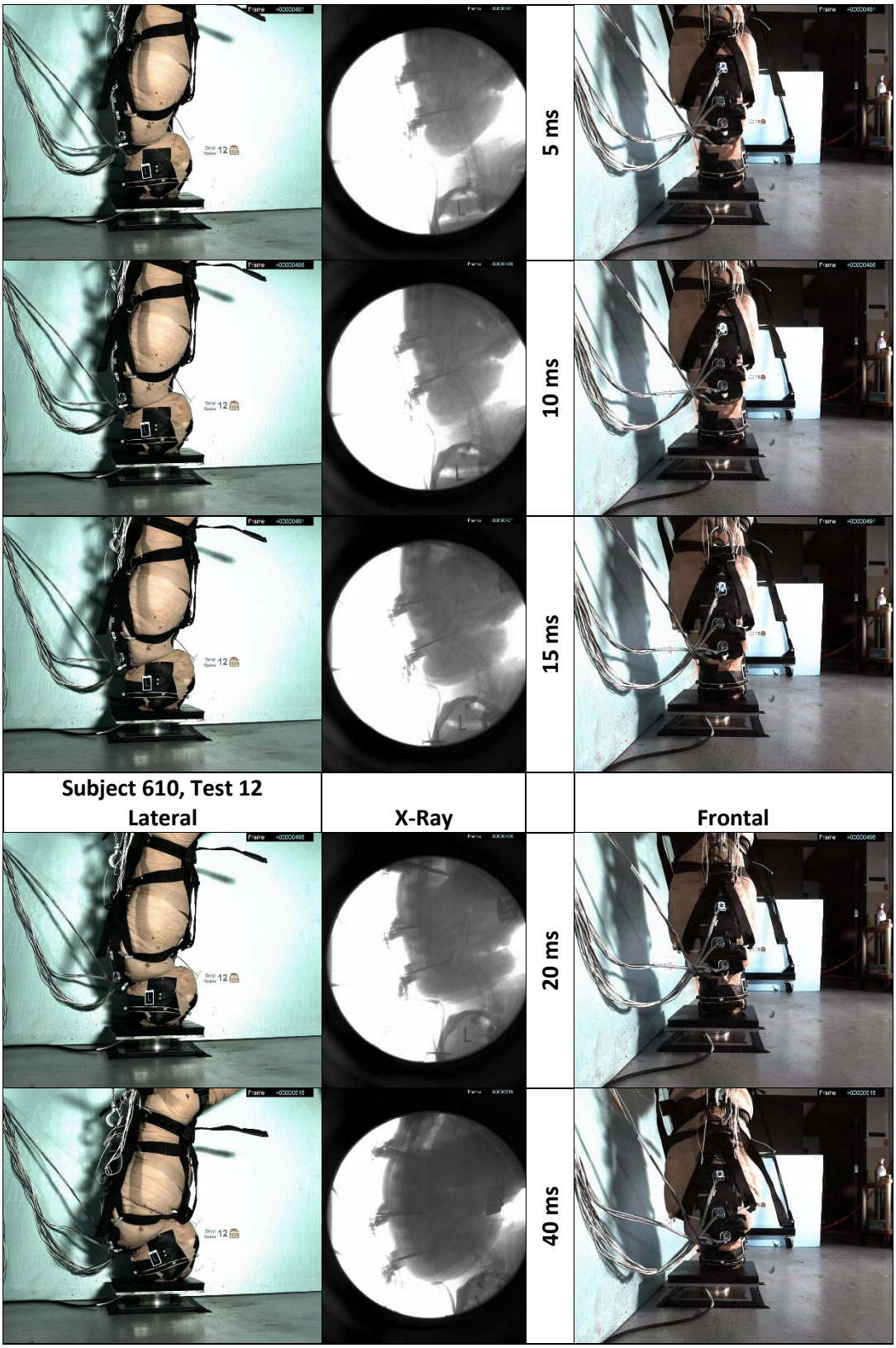
5 ms
10 ms
15 ms
Subject 610, Test 12
Lateral
X-Ray
Frontal
20 ms
40 ms

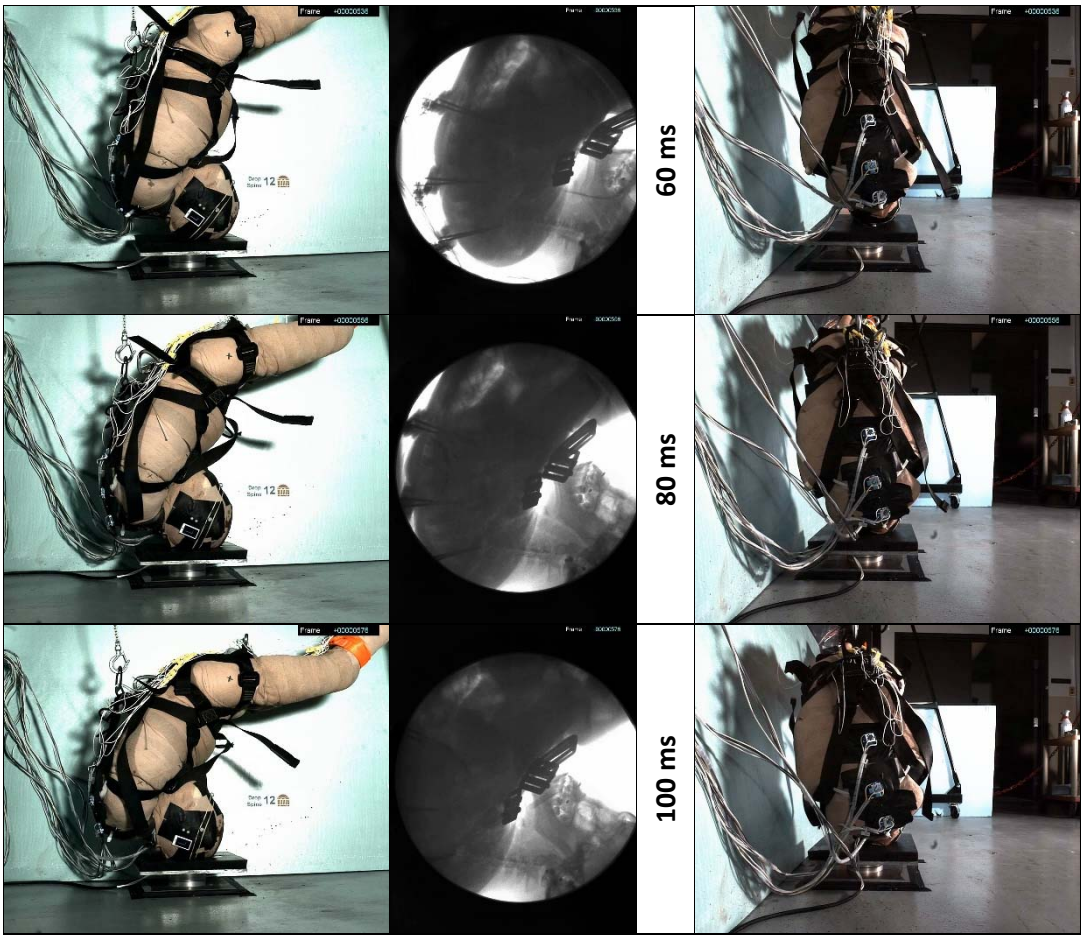

Subject 693, Test 13 Lateral	X-Ray		Frontal
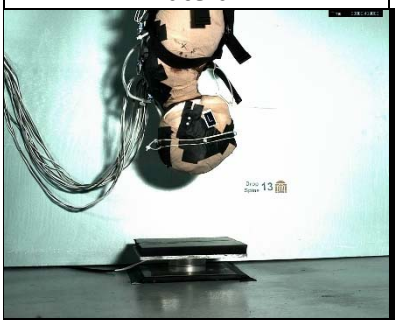	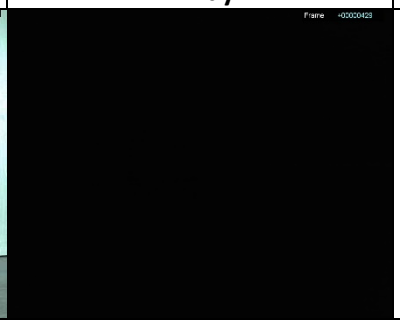	-50 ms	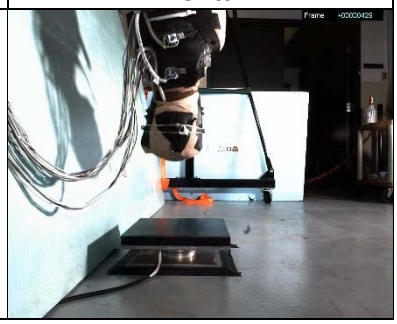

0 ms (contact)
5 ms
10 ms
15 ms
20 ms
Subject 693, Test 13
Lateral
X-Ray
Frontal

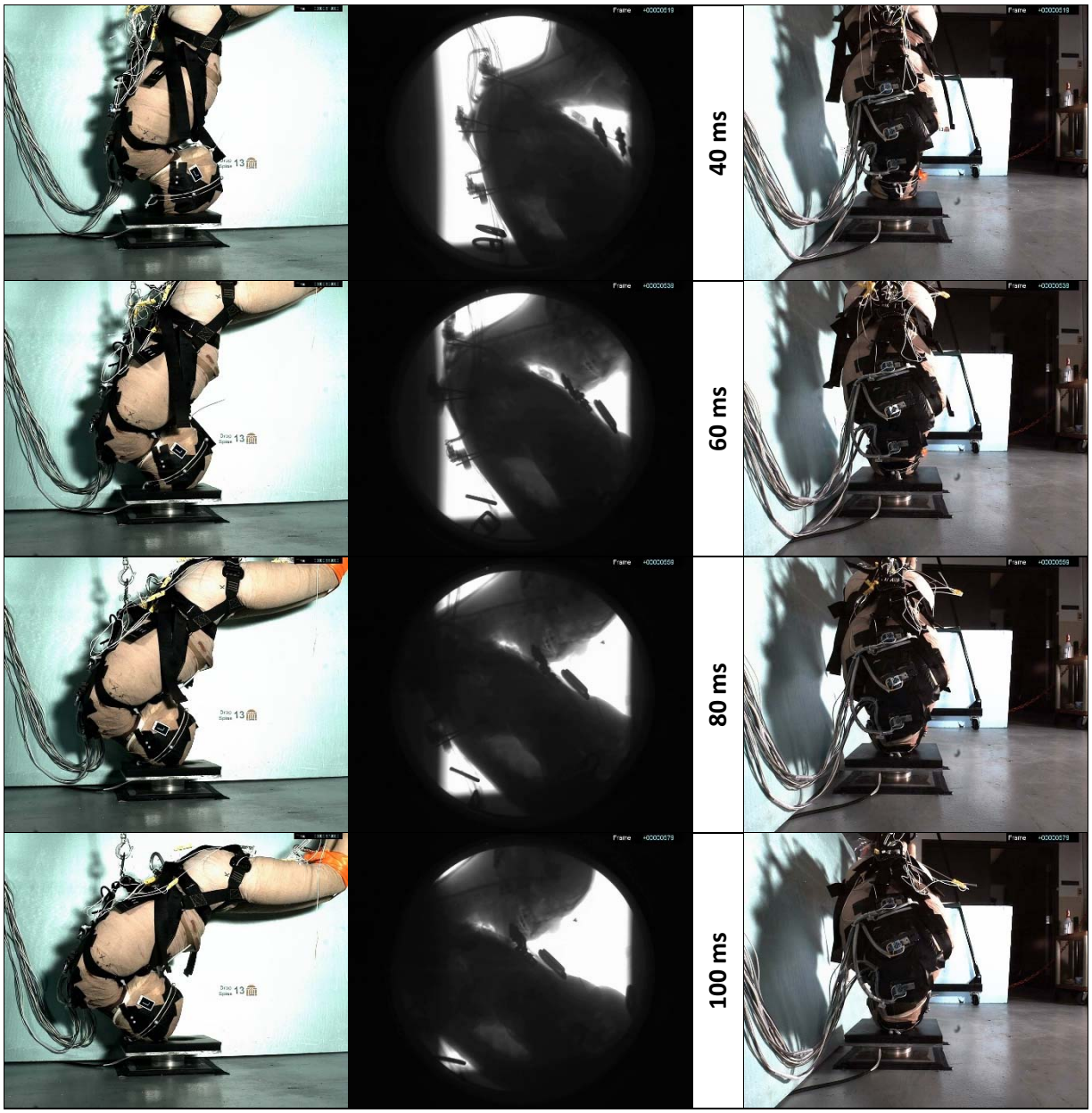
40 ms
60 ms
80 ms
100 ms